

Observation of a continuous phase transition in a shape-memory alloy

J. C. Lashley,¹ S. M. Shapiro,² B. L. Winn,³ C. P. Opeil,⁴ M. E. Manley,⁵ A. Alatas,⁶ W. Ratcliffe,⁷ T. Park,¹ R. A. Fisher,¹ B. Mihaila,¹ P. Riseborough,⁸ E. K. H. Salje,⁹ and J. L. Smith¹

¹*Los Alamos National Laboratory, Los Alamos, NM 87545, USA*

²*Brookhaven National Laboratory, Upton, NY 11973, USA*

³*Oak Ridge National Laboratory, Oak Ridge, TN 37831, USA*

⁴*Boston College, Department of Physics, 140 Commonwealth Avenue, Chestnut Hill, MA 02467, USA*

⁵*Lawrence Livermore National Laboratory, Livermore, CA 94550, USA*

⁶*Advanced Photon Source, Argonne National Laboratory, Argonne, IL 60439, USA*

⁷*National Institute of Standards and Technology, Gaithersburg, MD 20899, USA*

⁸*Department of Physics, Temple University, Philadelphia, PA 19122, USA*

⁹*Department of Earth Sciences, University of Cambridge, Downing Street, Cambridge CB2 3EQ, UK*

Elastic neutron-scattering, inelastic x-ray scattering, specific-heat, and pressure-dependent electrical transport measurements have been made on single crystals of AuZn and Au_{0.52}Zn_{0.48} above and below their martensitic transition temperatures ($T_M = 64$ K and 45 K, respectively). In each composition, elastic neutron scattering detects new commensurate Bragg peaks (modulation) appearing at $Q = (1.33, 0.67, 0)$ at temperatures corresponding to each sample's T_M . Although the new Bragg peaks appear in a discontinuous manner in the Au_{0.52}Zn_{0.48} sample, they appear in a continuous manner in AuZn. Surprising us, the temperature dependence of the Bragg peak intensity and the specific-heat jump near the transition temperature are in favorable accord with a mean-field approximation. A Landau-theory-based fit to the pressure dependence of the transition temperature suggests the presence of a quantum tricritical point in the AuZn phase diagram located at $T_M^* = 70.15$ mK and $p^* = 53.26$ kbar, with a quantum saturation temperature $\theta_s = 1.16 \pm 0.02$ K.

PACS numbers: 81.30.Kf, 71.20.Be,

A class of materials exhibiting martensitic (diffusionless) phase transformations yield properties used in a range of technological applications including implants to increase flow in restricted blood vessels [1], actuators for the treatment of high myopia [2], voltage generators [3], and orthodontic archwires [4]. These properties often depend on the history of the material and may allow it to recover its previous shape after deformation, known as the shape-memory effect (SME). It has long been recognized that these transformations are all thermodynamically first order (discontinuous) [5–7], regardless of the transition temperature. Special cases arise when the order parameter is coupled to an external field in a complicated way, leading to a weakly first-order transition [8], which are believed to result from a complicated coupling between strain and order parameter fluctuations. Because shape-memory alloys and other multiferroic materials owe their functionality to complicated cross-field responses between two (or more) pairs of conjugate thermodynamic variables, a description of the free-energy landscape and the ability to predict functionality become one and the same.

Phenomenological descriptions of the martensitic transformation pathway, based on reciprocal space [9] and real space [10] geometries, have established rules to determine relative twin and crystallographic orientations between the austenite (high-temperature) and martensite (low-temperature) modifications. Knowledge of the symmetry breaking allows for a definition of the energetic driving force in terms of the difference in free energies between phases. In the Ginzburg-Landau (GL) approach, the free energy, F , is expressed as a sum of symmetry invariants. In its simplest form, F is approximated by a polynomial expansion in even

powers of an order parameter, Q , as $F(Q) = aQ^2 + bQ^4 + cQ^6 + \frac{g}{2}|\nabla Q|^2$. For martensitic transformations, Q is taken to be strain or strain coupled to shuffle (displacements involving quasi-static phonons with fractional commensurate wave vectors with uniform shears [11]). The coefficients a, b, c, g are material parameters to be determined experimentally.

For the majority of shear-induced transformations, the GL expansion captures the essential physics [12, 13] such as constitutive response [14, 15] and the occurrence of anti-phase boundaries [16]. When applied to shape-memory alloys, the presence of intervening (premartensitic) phases [17], presents difficulties for both experiment and theory as to a unique characterization of the order parameter. Further issues have arisen in materials exhibiting quantum mechanical effects in the band structure and strong electron-phonon coupling [18]. In order to integrate these cases into GL theory, it is necessary to measure and access each thermodynamic property and infer cross-field couplings of the order parameter. The ability to distinguish between the subtle differences between first-order and weakly first-order depends on the ability to resolve the behavior of pertinent physical properties.

It was anticipated that a study of a simple ordered binary shape-memory alloy free of intervening phases at low temperatures could delineate fundamental features governing the discontinuous nature of a martensitic phase transformation. The AuZn system meets this criterion, showing no precursor phases and a low transition temperature ($T \leq 100$ K). In this Letter we examine the AuZn system for thermodynamic properties that contribute to the first-order or weakly first-order nature of the free-energy landscape. We measure elastic neutron-scattering, inelastic x-ray scattering, specific-

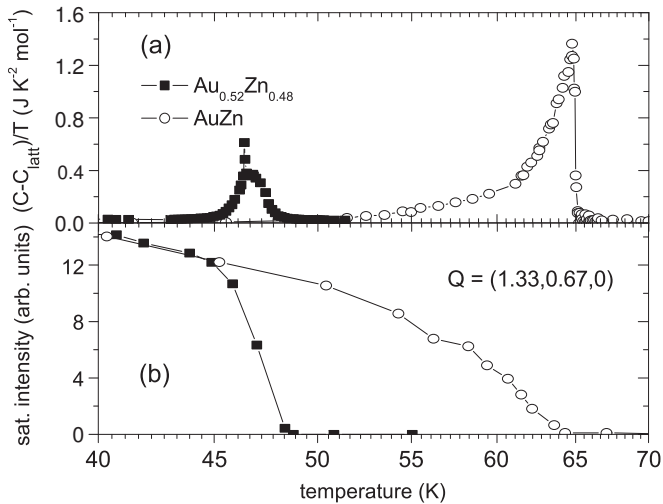


FIG. 1: (a) The excess specific heat divided by temperature versus temperature in the vicinity of the martensitic transitions for $\text{Au}_{0.52}\text{Zn}_{0.48}$ and AuZn . (b) Temperature dependence of the satellite-peak intensity along $Q = (1.33, 0.67, 0)$.

heat, and the pressure dependence of the transition by electrical transport. While we observed classical first-order behavior at 45 K for $\text{Au}_{0.52}\text{Zn}_{0.48}$, to our surprise and contrary to the definition of a martensitic transition we observed power-law behavior in AuZn near 64 K in the temperature dependence of the AuZn Bragg peak intensity and a sharp specific-heat jump. The power law yields favorable fits near T_M and yield a critical exponent consistent with mean-field theory.

Single crystals were prepared by fusion of the elements in a Bridgman furnace and were oriented by back-reflection Laue. The neutron experiments were performed on the BT9 triple-axis spectrometer at the NIST research reactor. Measurements of the phonon dispersion were made on XOR of sector 3 at the Advanced Photon Source, Argonne National Laboratory [19, 20]. Specific-heat measurements were measured using a thermal-relaxation calorimeter by Quantum De-

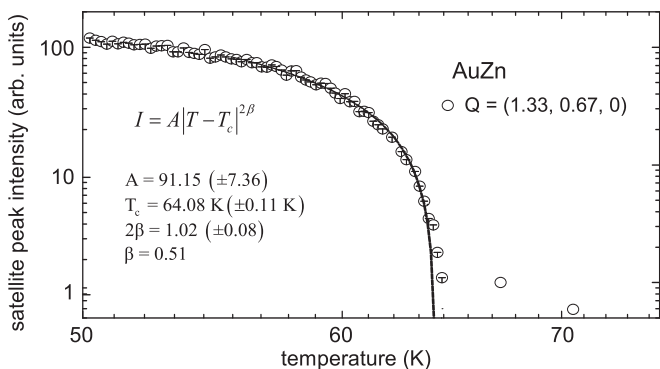


FIG. 2: Temperature dependence of the satellite peak intensity along $Q = (1.33, 0.67, 0)$ in AuZn , near the transition temperature. Empirical justification allows a fit to mean-field theory for $T \leq T_c$. Note the intensity axis is on a log scale.

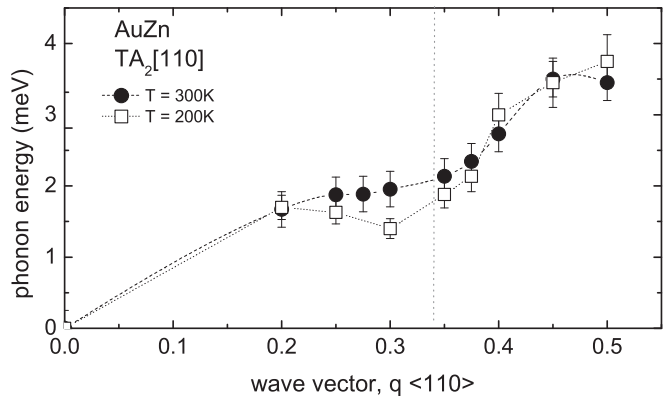


FIG. 3: Temperature dependence of the phonon dispersion in AuZn along the TA_2 branch. At 300 K one notices considerable phonon softening at $q = (0.33, 0.33, 0)$ (vertical line). The dashed lines between points are provided as guides to the eye.

sign [21]. The pressure dependence of the transition temperature was made by a four-terminal ac-transport method in a mechanical pressure cell designed to reach pressures of 30 kbar.

Previous investigations have shown that AuZn exhibits a martensitic transition as seen with low-temperature electron microscopy [22] and by recoverable transformation strain (shape-memory effect) [23]. Figure 1 shows the temperature dependence of (a) the excess specific heat and (b) the satellite peak intensity for $\text{Au}_{0.52}\text{Zn}_{0.48}$ and AuZn . Although we have measured the specific heat previously [24], it is plotted along with the elastic neutron-scattering data since it is revealing to compare both sets of measurements that were made on the same samples. The striking feature is the delta-like spike in the specific heat at 45 K for $\text{Au}_{0.52}\text{Zn}_{0.48}$, while there is a λ -anomaly at 64 K for AuZn . Because the specific-heat near the transition can be influenced by intrinsic defects, including triple defects and anti-structure defects known to be

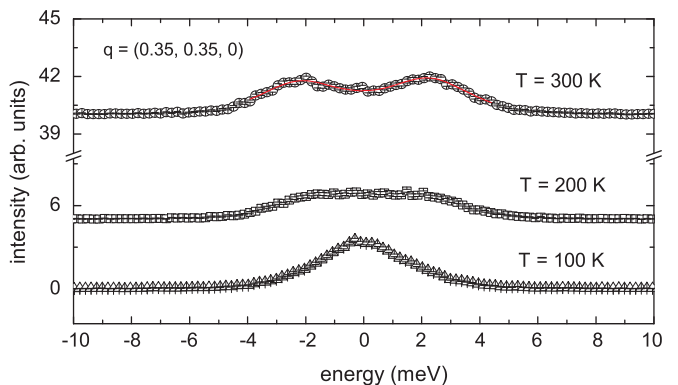


FIG. 4: (Color online) Inelastic x-ray scattering data showing the temperature dependence near the soft mode, $q = (0.35, 0.35, 0)$. The 300 and 200 K data are offset by 0.004 and 0.0005, respectively on the y-axis for clarity. The energy positions are fit to a double Lorentzian (solid curve) at 300 K to determine the phonon energy. The intrinsic resolution for inelastic x-ray scattering is 2 meV.

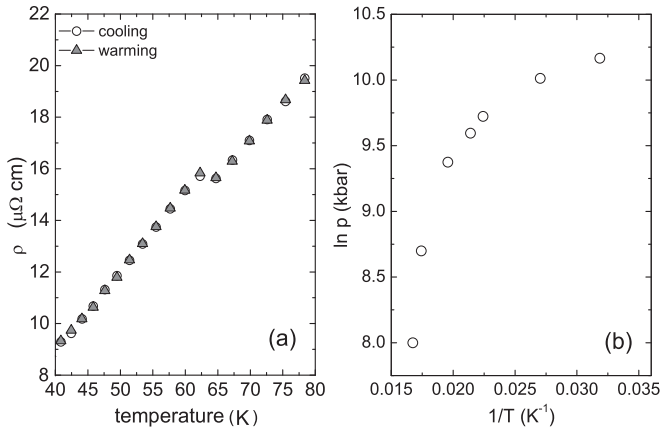


FIG. 5: (a) The electrical-resistivity data taken on cooling and warming is shown in the vicinity of T_M . (b) Plot of $\ln p$ versus $1/T$ to test the applicability Clausius-Clapeyron equation.

present in the B2 structure [25, 26], it was necessary to use a microscopic probe to determine whether or not the transition could be a broadened first-order transition. Elastic neutron-scattering measurements indicate that in each composition new commensurate Bragg peaks (modulation) appear at $Q = (1.33, 0.67, 0)$ at temperatures corresponding to each sample's T_M Figure 1(b). Mirroring the specific-heat data, the temperature dependence of the satellite peak intensity shows a rapid jump at 45 K in $\text{Au}_{0.52}\text{Zn}_{0.48}$, while a smooth mean-field like variation occurs for AuZn at 64 K. The satellite peak intensity is proportional to the square of the order parameter since it leads to the low-temperature rhombohedral phase. The specific-heat data also indicate thermal hysteresis (not shown) of 6 K at 45 K for $\text{Au}_{0.52}\text{Zn}_{0.48}$ and small hysteresis, difficult to measure, for AuZn at 64 K. The order parameter (squared) Fig. 1(b) curve for AuZn was measured by neutrons on heating and cooling, and unlike the specific-heat data Fig. 1 (a) we observe a small discontinuity and 1.5 K difference in transition temperature on cooling.

Based on these observations, we hypothesize that the transition at 64 K is not consistent with a first-order or weakly first-order transition but with a continuous transition. In order to test this hypothesis, we examine the satellite peak intensity curve for AuZn, Fig. 1(b), in more detail. Figure 2 shows the satellite peak intensity versus temperature in the vicinity of T_M for AuZn. Near the transition temperature, the satellite peak appears to evolve continuously with increasing temperature, showing a power-law temperature dependence given by $I = A|T - T_c|^{2\beta}$, where the satellite peak intensity is I , the critical temperature is T_c , and the critical exponent is β . The measured satellite peak intensity, I , was fit over a region where $T \rightarrow T_c$, as determined by Pippard's cylindrical-approximation to a λ -line [27]. We obtain $T_c = 64.08 \pm 0.11$ K and $2\beta = 1.02 \pm 0.08$ ($\beta = 0.51$). The value of the critical exponent obtained from the fit is close to the theoretic value 0.50, obtained for the mean value of the order parameter. In the present case, β is analogous to the van der Waals (liquid

+ gas) transition. One could argue that mean field exponents were obtained by coincidence given that the critical regime, as defined by the Ginzburg-criterion, is restricted to a range of temperatures too small to be resolved by our experiments, or that the correlation length does not diverge since it is limited by other extrinsic disorder (*i.e.*, martensite twins) or intrinsic fluctuations. The latter possibilities seems more plausible to us, since that the inverse correlation length, or width of the Bragg peaks (not shown), increase as the temperature is lowered below T_M .

As the temperature is lowered, the unit cell is distorted in the [110] shear direction. A commensurate shuffle of every third unit cell results in a hexagonal primitive unit cell formed from nine primitive cubic cells of the parent phase. This structure can also be described in terms of its conventional rhombohedral unit cell. In Fig. 3 we show the TA_2 phonon-dispersion curves along [110], measured by inelastic x-ray scattering at temperatures of 300 K and 200 K. The inflection in the phonon frequency near $\xi = 1/3$ indicates the low shear instability along the TA_2 [110] branch. This inflection is comparable to an earlier investigation [28] of off-stoichiometric AuZn samples. At 300 K, the phonon energy positions have been fit over the energy range $-4 \text{ meV} \leq E \leq 4 \text{ meV}$ to a double Lorentzian, as shown in Figure 4. The phonons continuously soften with decreasing temperature to the point that separation becomes difficult below 200 K.

In order to elucidate the order of the transition we looked for evidence of thermal hysteresis in the temperature dependence of the electrical resistivity. Figure 5 (a) shows the change in resistivity between cooling and warming, both rates were 0.2 K min^{-1} , of the change in resistivity. In the region of T_M there is no difference, to within experimental error. Because of the lack of hysteresis, we elected to measure the pressure dependence of the transition. For a first-order (liquid + gas) transition, the Clausius-Clapeyron relation, $\ln p/p_0 = -\Delta H/(RT) + A$, predicts a linear relationship for $\ln p/p_0$ versus $1/T$ with the slope $(-\Delta H/R)$. Here, p denotes the pressure, H the enthalpy, R the universal gas constant, and p_0 is a reference pressure. Figure 5(b) shows the plot of $\ln p$ versus $1/T$. It appears that there is no observable linear region and that the conditions for the applicability of the Clausius-Clapeyron relation are not met.

We use a modified GL free energy expression to describe the quantum saturation in the order parameter expected at sufficiently low temperature [29]. This saturation effect reflects the departure from classical behavior as the absolute temperature approaches zero and is a direct consequence of the third law of thermodynamics. Following Salje *et al.* [29], we fit the pressure dependence of the transition as $\theta_s/T_M(p) = \coth^{-1}[\coth(\theta_s/T_M(0)) - p/p_0]$. Here θ_s is a phenomenological temperature below which quantum mechanical effects are dominant. We choose $p_0 = 1$ kbar, and find $\theta_s = 1.1668 \pm 0.0236$ K. The resulting phase diagram predicts a quantum tricritical point at $T_M^* = 70.15$ mK and $p^* = 53.26$ kbar. Figure 6 depicts the experimental pressure dependence of the transition temperature for pressures up to

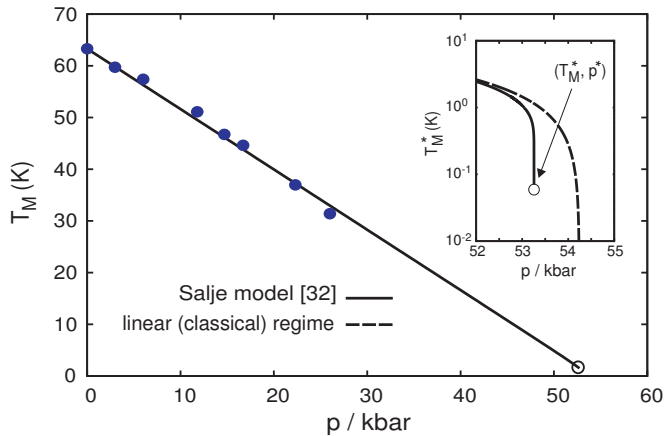


FIG. 6: (Color online) Pressure dependence of the transition temperature up to pressures of nearly 30 kbar, together with a fit to Salje's model [29] which accounts for quantum saturation effects close to zero absolute temperature. The difference between the linear (classical) and quantum-dominant behavior is illustrated in the inset. We find that quantum effects become important for temperatures lower than $\theta_s = 1.167 \pm 0.024$ K, and a quantum tricritical point is predicted at $T_M^* = 70.15$ mK and $p^* = 53.26$ kbar.

nearly 30 kbar, together with the fit to Salje's model and a linear fit of the data to characterize the classical regime. We find a classical (negative) slope of 1.1670 ± 0.0236 K, very close to the fitted value of θ_s , as expected. The difference between the classical and quantum regimes at temperatures of the order of θ_s is illustrated in the inset of Fig. 6.

To summarize, we report results of a detailed experimental study of the martensitic transition in AuZn. While the temperature dependence of the specific heat and the order parameter (squared) show marked first-order behavior at 45 K for $\text{Au}_{0.52}\text{Zn}_{0.48}$, we observed a continuous feature well-described by a mean-field exponent for AuZn at 64 K. The latter result is contrary to the established definition of a martensitic transition. Providing supporting evidence to the continuous nature of the phase transition in AuZn are the lack of thermal hysteresis from electrical-resistivity measurements and the disagreement of pressure data with the Clausius-Clapeyron relation. Using Salje's model to describe the quantum saturation effects close to zero absolute temperature, we predict the presence of a quantum tricritical point in the phase diagram located at $T_M^* = 70.15$ mK and $p^* = 53.26$ kbar, with a phenomenological temperature $\theta_s = 1.16 \pm 0.023$ K for the onset of quantum effects.

This work was performed under the auspices of the United States Department of Energy and Department of Commerce and supported in part by the Trustees of Boston College.

- [1] P. W. Duerig, MRS Bulletin **27**, 101 (2002).
- [2] I. Yu *et al.*, Mater. Sci. Eng. A **481-482**, 651 (2008).
- [3] I. Suorsa *et al.*, J. Appl. Phys. **95**, 8054 (2004).
- [4] J. Jafari, S. M. Zebarjad, and S. A. Sajjadi, Mater. Sci. Eng. A. **473**, 42 (2008).
- [5] R. C. Albers *et al.*, Comp. and Appl. Math. **23**, 345 (2004).
- [6] J. G. Boyd and D. C. Lagoudas, Int. J. Plasticity **12**, 805 (1996).
- [7] P. W. Gash, J. Appl. Phys. **54**, 6900 (1983).
- [8] S. Rubini and P. Ballone, Phys. Rev. B. **48**, 99, (1993).
- [9] J. S. Bowles and J. K. Mackenzie, Act. Met. **2**, 129 (1954).
- [10] M. S. Wechsler, D. S. Lieberman, and T. A. Read, J. of Metals **5**, 1503 (1953).
- [11] W.G. Burgers, Physica Utrecht **1**, 561 (1934).
- [12] P. Toledano and P. Toledano, The Landau Theory of Phase Transformations (World Scientific, Singapore, 1987).
- [13] E. K. H. Salje, Phase Transformations in Ferrelastic and Coelastic Solids (Cambridge University Press, Cambridge, UK, 1990).
- [14] R. Ahluwalia *et al.*, Acta. Mat. **52**, 209 (2004).
- [15] M. Iwata and Y. Ishibashi, J. Phys. Soc. Jap. **72**, 2843 (2003).
- [16] W. Cao, A. Saxena, and D. M. Hatch, Phys. Rev. B. **64**, 024106 (2001).
- [17] S. Kartha *et al.*, Phys. Rev. Lett. **67**, 3630 (1991).
- [18] K. H. Ahn *et al.*, Phys. Rev. B. **71**, 212102 (2005).
- [19] H. Sinn *et al.*, Nucl. Inst. and Meth. in Phys. Res. A **467**, 1545 (2001).
- [20] H. Sinn, J. Phys. Cond. Matter **13**, 7525 (2001).
- [21] J. C. Lashley *et al.*, Cryogenics **43**, 369 (2003).
- [22] H. Pops and T. B. Massalski, Trans. Met. Soc. AIME **223**, 728 (1965).
- [23] T. Darling *et al.*, Phil. Mag. B. **82**, 825 (2002).
- [24] R. McDonald *et al.*, J. Phys. Cond. Mat. **17**, L69 (2005).
- [25] Y. A. Chang and J. P. Neumann, Prog. Sol. St. Chem. **14**, 221 (1985).
- [26] D. Gupta and D. S. Lieberman, Phys. Rev. B. **4**, 1070 (1971).
- [27] A. B. Pippard, Phil. Mag. **1**, 473 (1956): The cylindrical approximation arises from the fact that, near the λ -line, the entropy surface may be regarded as cylindrical as the only significant curvature occurs on planes normal to the λ -line. Using this fact, the isobaric specific heat can be related to the volume coefficient of thermal expansion, β by $(\partial C_p / \partial T)_p = \phi V T_\lambda (\partial \beta / \partial T)_p$, where $\phi \equiv (\partial p / \partial T)_\lambda$. For a continuous transition, one expects a linear dependence over the temperature range where the cylindrical approximation holds in a plot of C_p versus β . Applying this approximation to the AuZn system, we obtain a linear region 7 K below the λ -transition temperature.
- [28] T. Makita *et al.*, Phys. B. **213**, 430 (1995).
- [29] S. A. Hayward and E. K. H. Salje, J. Phys.: Condens. Matter **10**, 1421 (1998); J. M. Pérez-Mato and E. K. H. Salje, *ibid.* **12**, L29 (2000).